



Canadian Journal of Fisheries and Aquatic Sciences

Escape, discard and landing probability of *Nephrops norvegicus* in the Mediterranean Sea creel fishery

Journal:	<i>Canadian Journal of Fisheries and Aquatic Sciences</i>
Manuscript ID	cjfas-2022-0190.R1
Manuscript Type:	Article
Date Submitted by the Author:	23-Nov-2022
Complete List of Authors:	Mašanović, Marina; University of Zagreb, Doctoral Study in Oceanology Herrmann, Bent; SINTEF Ocean, Fisheries Technology Brčić, Jure; University of Split, University Department of Marine Studies
Is the invited manuscript for consideration in a Special Issue? :	Not applicable (regular submission)
Keyword:	Creel size selection, <i>Nephrops norvegicus</i> , Mediterranean Sea, Pot size selection

SCHOLARONE™
Manuscripts

1 **Escape, discard and landing probability of *Nephrops norvegicus* in the**
2 **Mediterranean Sea creel fishery**

3
4 **Marina Mašanović^{a*}, Bent Herrmann^{b,c,d}, Jure Brčić^e**

5 ^a University of Zagreb, Doctoral study of Oceanology at Faculty of Science, Horvatovac 102a, 10 000 Zagreb,
6 masanovic.marina@gmail.com

7 ^b SINTEF Ocean, Brattørkaia 17C, N-7010, Trondheim, Norway, bent.herrmann@sintef.no

8 ^c UiT, The Arctic University of Norway, Breivika, N-9037, Tromsø, Norway.

9 ^d DTU Aqua, Denmark Technical University, Hirtshals, Denmark.

10 ^e University of Split, Department of Marine Studies, 21000, Split, Croatia jure.brcic@unist.hr

11
12 * Corresponding author. University of Zagreb, Doctoral study of Oceanology at Faculty of Science, Horvatovac 102a, 10 000 Zagreb; E-mail
13 address: masanovic.marina@gmail.com (M. Mašanović)

14

15

16

17

18

19

20

21

22

23

24

25

26

27

28

29

30

31 *Abstract*

32 Size selection in creel fishery consists of two processes: the first taking place in the creel on the
33 seabed and the second made by the fisher on the vessel. However, no study has ever considered
34 both processes when assessing the size selection in creel fisheries. This study presents a
35 framework for including both and demonstrates it to predict the effect of mesh size and shape
36 on the creel fishery targeting the Norway lobster (*Nephrops norvegicus*) in the Mediterranean
37 Sea. For this specific fishery, we demonstrate that both processes play a role in the overall size
38 selection. Furthermore, we predict an optimal creel mesh size, which potentially eliminates the
39 second process taking place on the vessel, while maintaining high efficiency for the first process
40 on the seabed for the targeted sizes of *Nephrops*. The approach here presented can be also
41 applied to other creel fisheries.

42
43 **Keywords:** Creel size selection, *Nephrops norvegicus*, Mediterranean Sea, Fisher size selection

44

45 *1. Introduction*

46 *Nephrops norvegicus* (hereafter referred to as *Nephrops*) is a deep-sea burrowing decapod
47 inhabiting the muddy bottoms (Hill et al. 1990; Johnson et al. 2013) of the northeast Atlantic
48 and the Mediterranean Sea (Johnson et al. 2013). It is considered as one of the most valuable
49 shellfish species in the Mediterranean Sea (Lolas et al. 2021). *Nephrops* is caught all over the
50 Mediterranean Sea, mostly by bottom trawlers (Morello et al. 2009), with the majority of the
51 catches occurring in the Ionian and Adriatic Sea (FAO-GFCM 2021). According to FAO (FAO
52 2020), *Nephrops* is overexploited in a large part of the Mediterranean Sea. The total catch of
53 *Nephrops* in the Mediterranean Sea in 2019 was 2613 t, which is the lowest catch since 1950

54 (FAO-GFCM 2021). Besides trawls, *Nephrops* are also harvested by creels (Morello et al. 2009;
55 Brčić et al. 2018a; Lolas et al. 2021; Petetta et al. 2021), passive fishing gears that attract
56 *Nephrops* using the bait placed inside them. They are designed to allow an easy entry while
57 making the escape difficult (Thomsen et al. 2010). Specifically, the meshes of the creels only
58 enable escape of *Nephrops* that are sufficiently small to pass through the meshes.

59 Compared to bottom trawls, creels are known to have a low ecological impact (Eno et al. 2001;
60 Adey 2007; Kopp et al. 2020) and on average catch larger *Nephrops* in a much better condition
61 (Eriksson 2006; Ridgway et al. 2006), yielding little or no bycatch (Morello et al. 2009; Brčić
62 et al. 2018a). By contrast, the *Nephrops* catch efficiency in creels is lower than in bottom trawls
63 (Morello et al. 2009). Since the EU is encouraging alternative types of fishing methods that
64 increase size and species selectivity or minimize the negative impact of fishing activities on the
65 marine environment (Regulation (EU) No 1380/2013), creels present a valid alternative to
66 bottom trawls. In the eastern Adriatic Sea (Croatian waters), fishers target *Nephrops* using the
67 rectangular metal frame creels covered with 36 mm or 40 mm square mesh netting (Croatian
68 Regulation NN 84/2015). The fishery is mainly conducted in the internal waters (channel area)
69 from March to November, and each fishing vessel is allowed to fish with maximum 300 creels
70 (Brčić et al. 2018a). They are deployed in a longline system, typically with 30 creels per
71 longline, using small scale fishing vessels, and are usually retrieved after one or more days
72 (Brčić et al. 2018a). The average duration of retrieval process of one longline is less than 15
73 min (Brčić et al. 2018a). During this short period of time, the fisher takes the catch out of each
74 creel, sorts it, rebaits all creels and prepares them for the next deployment. During the catch
75 sorting process, the fisher must quickly evaluate the size of each *Nephrops* to minimize the air
76 and light exposure of each undersized *Nephrops* (MCRS = 20 mm carapace length CL; Council
77 Regulation (EC) No 1967/2006) before returning it back to the sea alive, since *Nephrops* caught
78 with creels is exempt from the landing obligation because of high survival rates (Commission

79 Delegated Regulation (EU) 2018/3036). This represents a second size selection process,
80 operated by the fisher. However, this process could be avoided if the size selection of creels on
81 the seabed is optimized with respect to a desired exploitation pattern. This demonstrates the
82 importance of considering both the gear and fisher size selection when evaluating a fishery, as
83 has been shown for trawls (Mytilineou et al. 2018; 2020; 2021a; 2021b). Therefore, these two
84 selection processes should be considered when making management decisions regarding the
85 gear regulations for a specific fishery. Hence, our main goal was to present a framework that
86 includes both the gear and fisher size selection and use them to predict the effect of mesh size
87 and shape on the creel fishery targeting *Nephrops* in the Mediterranean Sea.

88

89 **2. Material and methods**

90 *2.1 Experimental design*

91 The sea trials were conducted between the 5th of April and the 4th of July 2019 in the North
92 Adriatic Sea (Figure 1) onboard a commercial small scale fishing vessel (LOA 5.60 m and
93 engine power 22 kW). An observer followed the fisher during his usual fishing operation. The
94 commercial creels deployed by the fisher were made of plastic-coated rectangular metal frame
95 (length 700 mm, width 410 or 450 mm, depth 270 mm and Ø5 mm) mounted with a diamond
96 mesh polyamide netting with opening angle of 90° to obtain a square mesh shape (hereafter
97 referred as to test creels). The mean mesh size of the test creels was 34.89 ± 0.46 mm SD and
98 the mean opening angle $82.15^\circ \pm 5.61^\circ$ SD. On each fishing day, in addition to all test creels
99 deployed by the fisher, a special permit was obtained for one control longline containing creels
100 identical in size and design (Supplement; Figure S1), apart from being mounted with a smaller
101 mesh size netting (hereafter referred as to control creels), following the methodology described
102 in Brčić et al. (2018a). The mean mesh size of the control creels was 15.7 ± 0.47 mm SD and

103 mean opening angle $85.50^\circ \pm 5.30$ SD. The mesh size of both, test and control creels were
 104 measured with the OMEGA mesh gauge and the opening angle using the image analysis routine
 105 implemented in FISHSELECT software (Herrmann et al., 2013). Both types of creels had two
 106 conical entrances positioned opposite each other, with a hook in the middle for attaching the
 107 bait. All creels were baited with the same quantity of saddled seabream *Oblada melanura*. They
 108 were deployed in a longline system, with 29 to 40 creels attached to the mainline, and retrieved
 109 after one to four days, depending on the weather conditions. Upon retrieval, the fisher sorted
 110 the catch of each longline into two groups, one destined to be discarded and the other to be
 111 landed. The observer onboard the vessel recorded whether each *Nephrops* belonged to the
 112 discard or landing portion of the catch. The observer also measured their CL to the nearest mm
 113 and registered the count number for each 1 mm CL class.

114

115 2.2 Data analysis

116 2.2.1 Creel size selection

117 Due to relatively small catches per creel, the catch from one longline deployment was
 118 considered as the base unit in the subsequent analysis (Brčić et al. 2018a). Given that the
 119 experimental data collection included test and control creels and since there was no obvious
 120 way of pairing the data, test creel selectivity was estimated following the unpaired estimation
 121 methodology described in Brčić et al. (2018a). The analysis was performed separately for
 122 deployments with different soak times by minimizing the following expression with respect to
 123 parameters v_{creel} and SP :

$$124 - \sum_{CL} \left\{ \sum_{i=1}^a n_{TCLi} \times \ln \left(\frac{SP \times r_{creel}(CL, v_{creel})}{SP \times r_{creel}(CL, v_{creel}) + 1 - SP} \right) + \sum_{j=1}^b n_{CCLj} \times \ln \left(1.0 - \frac{SP \times r_{creel}(CL, v_{creel})}{SP \times r_{creel}(CL, v_{creel}) + 1 - SP} \right) \right\} \quad (1)$$

125 where v_{creel} is a vector of parameters describing the size selection model $r(CL, v_{creel})$, nT_{CLi} and
 126 nC_{CLj} represent the number of *Nephrops* of carapace length CL retained by i -th and j -th
 127 deployment from the total of a test and b control creel deployments, respectively. The
 128 probability that *Nephrops* of carapace length CL would enter either test or control creel was
 129 modelled using the split parameter SP , where SP represents the probability that *Nephrops*
 130 entered the test creel and $1-SP$ represents the probability that it entered the control creel,
 131 conditioned that it entered one of them (Wileman et al. 1996). Given that creels were mounted
 132 with a single size mesh netting and based on the previous studies (Xu and Millar 1993; Winger
 133 and Walsh 2011; Brčić et al. 2018a; Olsen et al. 2019), we assumed that size selection in creels
 134 can be described using the following *logit* model:

$$135 \quad r_{creel}(CL, v_{creel}) = \frac{\exp\left(\frac{\ln(9)}{SR_{creel}} \times (CL - CL50_{creel})\right)}{1.0 + \exp\left(\frac{\ln(9)}{SR_{creel}} \times (CL - CL50_{creel})\right)} \quad (2)$$

136 where v_{creel} represents the vector of parameters $CL50_{creel}$ and SR_{creel} . $CL50_{creel}$ is the CL of a
 137 *Nephrops* that has a 50% probability of being retained by the test creel given that it entered it.
 138 SR_{creel} is the difference in the CL of *Nephrops* with a 75% and 25% probability, respectively,
 139 of being retained by the test creel, given that it entered it. The estimation of the average
 140 selectivity for the test creel with *logit* size selection model (2) requires finding the values of the
 141 parameters SP , $CL50_{creel}$ and SR_{creel} that minimize (1). Minimizing the expression (1) is
 142 equivalent to maximizing the likelihood for the experimental data.

143 The ability of the model to describe the experimental data was inspected visually and evaluated
 144 based on the p -value and model deviance versus the degrees of freedom (DOF). Fit statistics is
 145 considered to be poor when p -value < 0.05 and deviance/DOF $\gg 1$. In case of poor fit statistics,
 146 the residuals were inspected to determine if this is due to structural problems or due to the
 147 overdispersion in the data (Wileman et al. 1996).

148 The double bootstrap method for unpaired data (Sistiaga et. al. 2016; Brčić et al. 2018a) was
149 used to estimate the 95% confidence intervals for the size selection curve and the associated
150 parameters. This method accounted for the within deployment variation in *Nephrops* size
151 structure as well as for the between deployment variation in the availability of *Nephrops* on the
152 fishing grounds and the between deployment variation in creel size selection. A total of 1000
153 bootstrap repetitions were conducted to calculate the 95% Efron percentile confidence intervals
154 (Efron 1982) for the size selection curves and their parameters.

155 The analysis above was performed separately for deployments with different soak times. To
156 determine if there is a length-dependent difference in retention probability ($\Delta r(CL)$) between
157 deployments with different soak times (x, y), the delta method (Larsen et al. 2018, Mytilineou
158 et al. 2020; 2021b) was used as follows:

$$159 \quad \Delta r(CL) = r_x(CL) - r_y(CL) \quad (3)$$

160 The $r_x(CL)$ and $r_y(CL)$ represent the retention probabilities obtained for deployments with x and
161 y day soak time, respectively. Following Larsen et al. (2018) and Olsen et al. (2019), the 95%
162 Efron confidence intervals for each $\Delta r(CL)$ were estimated based on the bootstrap population
163 of results obtained for $r_x(CL)$ and $r_y(CL)$ as follows:

$$164 \quad \Delta r(CL)_i = r_x(CL)_i - r_y(CL)_i \quad (4)$$

165 where i represents the bootstrap repetition index (1 to 1000). Since the bootstrap file generated
166 for each soak time was independent, it was possible to obtain a bootstrap file for the difference
167 in retention probability for deployments with different soak times (Larsen et al. 2018; Olsen et
168 al. 2019). The results of the delta method were visualized through delta plots (Larsen et al.
169 2018; Olsen et al. 2019). If the 95% Efron confidence intervals for the $\Delta r(CL)$ in the delta plot
170 include 0.0, this would mean that there is no significant difference in the length-dependent

171 retention probability between the two deployments with different soak times. In case this was
 172 true for all $\Delta r(CL)$, the data from all deployments, irrespective of the soak time, were pooled
 173 and an additional creel selectivity analysis on the pooled data was performed.

174 2.2.2 Fisher size selection

175 Once the catch retained by the creels of each longline is brought onboard the fishing vessel, the
 176 second selection process begins with the fisher sorting *Nephrops* into two groups: discard and
 177 landing. The data collected in this way can be treated as cover codend data (Wileman et al.
 178 1996). Specifically, each *Nephrops* of CL discarded by the fisher was considered as an escapee,
 179 while each landed *Nephrops* was considered as retained. Hence, the data from each deployment
 180 contained information on the number of discarded and landed *Nephrops* of each CL . The
 181 analysis was then performed by minimizing the following expression:

$$182 \sum_{i=1}^{a+b} \sum_{CL} \{nL_{CLi} \times \ln(r_{fisher}(CL, \mathbf{v}_{fisher})) + nD_{CLi} \times \ln(1 - r_{fisher}(CL, \mathbf{v}_{fisher}))\} \\ 183 \quad (5)$$

184 where nL_{CLi} and nD_{CLi} represent the number of *Nephrops* of CL landed and discarded by the
 185 fisher, respectively, from i -th deployment, from the total of $a+b$ longline deployments. The
 186 following *logit* size selection model can then be fitted to the data to obtain a fisher size selection
 187 curve:

$$188 r_{fisher}(CL, \mathbf{v}_{fisher}) = \frac{\exp\left(\frac{\ln(9)}{SR_{fisher}} \times (CL - CL50_{fisher})\right)}{1.0 + \exp\left(\frac{\ln(9)}{SR_{fisher}} \times (CL - CL50_{fisher})\right)} \quad (6)$$

189 where \mathbf{v}_{fisher} represents the vector of parameters ($CL50_{fisher}$ and SR_{fisher}). The $CL50_{fisher}$ represents
 190 the CL of a *Nephrops* that has a 50% probability of being landed by the fisher given that it has
 191 been retained by the creel. The SR_{fisher} is the difference in CL of a *Nephrops* with a 75% and
 192 25% probability, respectively, of being landed by the fisher, given that it has been retained by

193 the creel. Therefore, the estimation of the average fisher selectivity with the *logit* size selection
 194 model (6) requires finding the values of the parameters $CL50_{fisher}$ and SR_{fisher} that minimize (5).
 195 The ability of the model to describe the experimental data was inspected following the same
 196 procedure as described for the creel size selection models.

197 2.2.3 Estimating the experimental length-dependent escape, landing and discard probability

198 Inspired by the work of Mytilineou et al. (2018), once the creel and fisher size selection have
 199 been estimated, it was possible to combine these two sequential processes to model the overall
 200 size selection for *Nephrops* in the given creel fishery. Once *Nephrops* of CL enters one of the
 201 test creels, three outcomes are possible:

- 202 1) *Nephrops* can escape through creel meshes described by the probability $P_{esc}(CL, \mathbf{v}_{creel})$,
- 203 2) *Nephrops* can be retained by the creel but discarded by the fisher, described by the probability
 204 $P_{disc}(CL, \mathbf{v}_{creel}, \mathbf{v}_{fisher})$, and
- 205 3) *Nephrops* can be retained by the creel and landed by the fisher, described by the probability
 206 $P_{land}(CL, \mathbf{v}_{gear}, \mathbf{v}_{fisher})$.

207 All three probabilities were then, following Mytilineou et al. (2018), modelled as:

$$208 P_{esc}(CL, \mathbf{v}_{creel}) = 1.0 - r_{creel}(CL, \mathbf{v}_{creel})$$

$$209 P_{disc}(CL, \mathbf{v}_{creel}, \mathbf{v}_{fisher}) = r_{creel}(CL, \mathbf{v}_{creel}) \times (1.0 - r_{fisher}(CL, \mathbf{v}_{fisher})) \quad (6)$$

$$210 P_{land}(CL, \mathbf{v}_{creel}, \mathbf{v}_{fisher}) = r_{creel}(CL, \mathbf{v}_{creel}) \times r_{fisher}(CL, \mathbf{v}_{fisher})$$

211 Once the length-dependent discard probability was estimated, the following set of discard
 212 indicators (Mytilineou et al. 2018; 2021b) were also estimated: LDp_{max} representing the CL of
 213 *Nephrops* where maximum discarding probability (Dp_{max}) occurs and DR_x representing the size
 214 range where discarding probability is at least $x\%$, where $x = (5\%, 25\%, 50\%, 75\%, 95\%)$. For

215 the details regarding the above-mentioned indicators, see Figure S2 in Supplement. The 95%
216 Efron confidence intervals were estimated using the double bootstrap method as described
217 previously in the text.

218

219 *2.2.4 Predicting the escape, discard and landing probability with different creel mesh sizes and* 220 *shapes*

221 The estimated experimental escape, discard and landing probabilities are specific for the test
222 creels used in the study. However, we were interested to find out how the escape, discard and
223 landing probabilities would change if creels with different mesh sizes and mesh opening angles
224 were used. Assuming that the average fisher size selection ($r_{fisher}(CL, \nu_{fisher})$) is constant, the
225 CREELSELECT model developed by Brčić et al. (2018b) was used to predict creel size
226 selection ($r_{creel}(CL, \nu_{creel})$) for different mesh sizes and mesh opening angles. As shown by Brčić
227 et al. (2018b), this model was able to accurately reproduce the experimental *Nephrops* creel
228 size selection obtained by Brčić et al. (2018a). In the present study, before making any
229 predictions, we first tested the model to see if it was able to reproduce the experimentally
230 obtained size selection curve for the test creels obtained in this study. The obtained values were
231 then used in the model (see Eq. S1 and Table S1 in the supplementary material for the details
232 of the model) to predict creel size selectivity. The predicted curve was then plotted together
233 with the experimentally obtained size selection curve from this study to check if the predicted
234 curve falls within the 95% Efron confidence intervals of the experimental curve. This would
235 provide an additional validation of the CREELSELECT model which can be used with
236 increased confidence to predict the creel size selection ($r_{creel}(CL, \nu_{creel})$) for *Nephrops*. The
237 legislated mesh sizes in Croatian *Nephrops* creel fishery are 36 or 40 mm (depending on the
238 region) and the deviation in mesh opening angle from the perfect square (opening angle =90°)

239 of $\pm 10\%$ is tolerated. Therefore, the model was used to predict $r_{creel}(CL, \mathbf{v}_{creel})$ for mesh sizes
 240 ranging from 30 mm to 46 mm in steps of 2 mm and opening angles ranging from 60° to 90° in
 241 steps of 2° . These predictions were then used together with the experimentally obtained r_{fisher}
 242 $(CL, \mathbf{v}_{fisher})$ (assuming it is constant) in (6) to predict the length-based escape, discard and
 243 landing probability in creels for the selected combination of mesh sizes and mesh opening
 244 angles. Further, based on the predicted length-dependent discard probability curves, we
 245 calculated a maximum discarding probability (Dp_{max}) for each combination of mesh size and
 246 mesh opening angle. The calculated Dp_{max} values were then visualized in an iso- Dp_{max} plot.

247

248 2.2.5 Predicting the effect of creel mesh size and mesh opening angle on *Nephrops* exploitation 249 pattern

250 To examine how applying different creel mesh sizes and opening angles would affect the
 251 exploitation pattern in the *Nephrops* creel fishery, the following set of indicators were
 252 calculated (Herrmann et al. 2021):

$$\begin{aligned}
 nP_{-} &= 100 \times \frac{\sum_{CL < MCRS} \{r(CL, CL50, SR) \times nPop_{CL}\}}{\sum_{CL < MCRS} \{nPop_{CL}\}} \\
 nP_{+} &= 100 \times \frac{\sum_{CL > MCRS} \{r(CL, CL50, SR) \times nPop_{CL}\}}{\sum_{CL > MCRS} \{nPop_{CL}\}} \quad (7) \\
 nDRatio &= 100 \times \frac{\sum_{CL < MCRS} \{r(CL, CL50, SR) \times nPop_{CL}\}}{\sum_{CL} \{r(CL, CL50, SR) \times nPop_{CL}\}}
 \end{aligned}$$

254 The $r(CL, CL50, SR)$ represents the size selection curve obtained for a specific combination of
 255 the creel mesh size and mesh opening angle predicted using the CREELSELECT model (Brčić
 256 et al. 2018b). The $nPop_{CL}$ represents the population size structure of *Nephrops* encountered
 257 during the sea trials. In this study, the size structure of the *Nephrops* population retained by the
 258 control creel was used as $nPop_{CL}$. The nP_{-} and nP_{+} , respectively, quantify the percentage of
 259 *Nephrops* individuals retained by the test creels below and above the Minimum Conservation

260 Reference Size ($MCRS$) from the population of *Nephrops* encountered during the sea trials
261 ($nPop_{CL}$). The $nDRatio$ (discard ratio) quantifies the proportion of *Nephrops* under $MCRS$ from
262 the total catch retained by the test creels. According to the regulation (Council Regulation (EC)
263 No 1967/2006), the $MCRS$ for *Nephrops* is 20 mm CL. However, in case the fisher discards a
264 certain portion of *Nephrops* above $MCRS$ (indicated by $CL50_{fisher} > MCRS$), then substituting
265 $MCRS$ with $CL50_{fisher}$ in (7) allows finding the optimum combination of the creel mesh size and
266 mesh opening angles that best match the exploitation pattern desired by the fisher. The preferred
267 values of nP^- and $nDRatio$ are those close to 0% and of nP^+ those close to 100% as possible
268 (Wienbeck et al. 2014; Sala et al. 2016; Brčić et al. 2018c; Kalogirou et al. 2019; Melli et al.
269 2020; Herrmann et al. 2021).

270 All the analyses were performed using the SELNET software (Herrmann et al. 2012; 2013).
271 The statistical software tool R (version 4.1.1; R Core Team 2021) was used to produce plots
272 using the metR (Campitelli 2021) and ggplot2 packages (Wickham 2016).

273

274 3. Results

275 A total of 7306 *Nephrops* were caught using 126 test and 15 control longlines during the 17
276 days of experimental fishing (Table 1). The longlines were deployed on the average depth of
277 77 m (± 6.98 SD). The CL of retained *Nephrops* individuals ranged from 24 to 65 mm in test
278 creels, and 17 to 59 mm in control creels. The mean number of individuals caught by test and
279 control longlines were 52.9 (± 13.6 SD) and 46.6 (± 8.9 SD), respectively. The structure of the
280 population caught in test and control longlines is shown in Figure S3 in Supplement.

281 To estimate the creel size selection for deployments retrieved after one (S1), two (S2), three
282 (S3) and four (S4) days, we performed the analysis in two steps. The first step included fitting

283 the logit curve (2) to the catch data. By visually inspecting the fit of the logit curve to
284 experimental catch data for the control and test creels summed over all deployments (the catch
285 sharing plot), it was noted that the fit was poor for the largest *Nephrops* length classes,
286 confirmed by fit statistics in most cases. Therefore, in the second step, all *Nephrops* above 40.69
287 mm CL were excluded from the analysis. The cut-off point (=40.69 mm CL) was obtained by
288 predicting the $CL_{99_{creel}}$ (the CL of a *Nephrops* that has a 99% probability of being retained by
289 the test creel given that it entered it) for the largest measured mesh size 36 mm + 2SD +10 mm
290 and OA = 90° using the CREELSELECT model (Brčić et al. 2018b). This has been done to
291 ensure that absolutely no *Nephrops* of that size could have escaped through the test creel
292 meshes. After this step, a visual inspection of the fit to experimental data for deployments
293 retrieved after one (S1), two (S2), three (S3) and four (S4) days indicated a good fit (Figure 2),
294 confirmed by fit statistics (Table 2).

295 The 95% Efron confidence intervals in the delta plots (Supplement; Figure S4) included 0.0 in
296 all cases, showing no significant difference in the length-dependent retention probability
297 between deployments with different soak times. This allowed performing an additional analysis
298 based on all deployments pooled together. The fit of the logit curve to the pooled experimental
299 data (Figure 3) shows a good fit, confirmed by the fit statistics in Table 3. The estimated pooled
300 $CL_{50_{creel}}$ and SR_{creel} values, together with their respective 95% confidence intervals, are
301 presented in Table 3. The estimated SP value is close to expected since there was a marked difference
302 between the number of test and control creels deployed.

303 The fisher size selection was modelled using the logit size selection curve shown in Figure 4.
304 The model reflected the trend in experimental data well. However, fit statistics (Table 3)
305 potentially indicated that the model was inappropriate for describing the experimental data.
306 Since no systematic patterns were observed after inspecting the residuals of the fit, the poor fit
307 statistics was ascribed to the overdispersion in the data (Wileman et al. 1996). Therefore, we

308 were confident in using this model to describe the fisher size selection. The estimated $CL50_{fisher}$
309 and SR_{fisher} values, together with their respective 95% confidence intervals, are presented in
310 Table 3. The $CL50_{fisher}$ was significantly larger than $CL50_{creel}$ (no overlap between their
311 respective 95% Efron confidence intervals) and the *Nephrops* $MCRS$ (=20 mm CL).

312 The two sequential selection processes by the gear and the fisher were combined to model the
313 overall size selection for *Nephrops* population entering the creel according to equation (6).
314 Figure 5. shows the S-shaped curves for the escape and landing probability as well as a bell-
315 shape discard probability curve. The left-hand side of the discard probability curve is defined
316 by the probability of escaping from the gear on the seabed, while the right-hand side of the
317 curve is defined by the fisher size selection. The maximum average discard probability of 83%
318 was estimated for *Nephrops* CL 28.26 mm (Table 3), which is significantly larger than the
319 *Nephrops* $MCRS$ (=20 mm CL). The overall size selection combining the creel and fisher
320 retention probability is represented by the landing probability (Figure 5).

321 To predict how the escape, discard and landing probabilities would change if creels with
322 different mesh sizes and mesh opening angles were used, we first had to inspect if the
323 CREELSELECT model (Brčić et al. 2018b) can accurately reproduce the experimentally
324 obtained creel size selection obtained in this study. The mean mesh size (=34.89 mm) and mean
325 opening angle (=82.15°) obtained from the creels used in experimental fishing in this study
326 were applied in the CREELSELECT model to make a prediction that can be compared with the
327 experimentally obtained size selection curve. The predicted curve falls within the 95% Efron
328 confidence intervals of the experimentally obtained curve (Supplement; Figure S5),
329 demonstrating that the CREELSELECT model can be used with confidence to predict
330 *Nephrops* size selection in creels.

331 After validation, the CREELSELECT model was used to predict the creel retention
332 probabilities for mesh sizes ranging from 30 mm to 46 mm in steps of 2 mm and opening angles
333 ranging from 60° to 90° in steps of 2°. The predicted probabilities were then used together with
334 the experimentally obtained fisher size selection probability to predict the length-dependent
335 escape, discard and landing probability in creels for the selected combination of mesh sizes and
336 mesh opening angles (Figure 6). From the Figure 6, it is evident that both mesh size and mesh
337 opening angle influence the escape, discard and landing probability of *Nephrops* in creels.

338 The Figure 7 shows the predicted maximum discard probabilities for creels as a function of
339 mesh size and opening angle. The plot can be used by fisheries managers to determine the right
340 combination of mesh sizes and opening angles for achieving the acceptable discard probability.

341 For instance, knowing that the legislation allows $\pm 10\%$ deviation from the perfect square shape
342 (opening angle = 90°), from the Figure 7, it is evident that the largest mesh size allowed in
343 Croatian waters (=40 mm) has a lower discard probability compared to the smallest mesh size
344 allowed (=36 mm). This is confirmed by the iso plots (Figure 8) showing the predicted
345 exploitation pattern indicators (nP^- , nP^+ , $nDRatio$) for the same mesh sizes and mesh opening
346 angles.

347 From the Figure 8, it is evident that the mesh size 36 mm with the opening angle 90° would
348 retain all sizes of *Nephrops* ($nP^+ > 99\%$) desired by the fisher ($>L50_{fisher}$). However, it would
349 also capture a substantial amount of *Nephrops* below this size ($nP^- \approx 20\%$) if exposed to a
350 population structure similar to that obtained by the control creel in this study. Therefore,
351 resulting discard ratio for this given mesh size and shape would be approximately 4%. The
352 mesh size 40 mm with the opening angle 90° would retain almost all sizes of *Nephrops* (nP^+

353 $\approx 92\%$) desired by the fisher ($\geq L50_{fisher}$) and only few below this size ($nP \approx 1\%$). Therefore,
354 the resulting discard ratio ($nDRatio$) would be $<1\%$.

355

356 4. Discussion

357 This is the first study that investigates the overall size selection of creels in the Mediterranean
358 *Nephrops* creel fishery considering both the gear and fisher size selection. The results from the
359 study demonstrate that both processes should be considered as they influence the gear
360 exploitation pattern. Therefore, the fisheries managers need to consider both processes when
361 making decisions regarding the gear regulations for this specific fishery. The methodology used
362 in this study has previously been applied in trawl fisheries (Mytilineou et al. 2018; 2020; 2021a;
363 2021b) and has the potential to be applied in other fisheries as well where the sorting process
364 is done manually by the fisher, e.g. creel fisheries targeting snow crab (Winger and Walsh 2007;
365 Olsen et al. 2019). Future selectivity studies should also consider fisher size selection, and the methods
366 presented here demonstrate how this could be addressed. Therefore, the application of such method
367 could potentially affect how size selectivity in such fisheries could be evaluated in the future.
368 Regarding the results obtained for the specific fishery investigated in this study, the average
369 $CL50_{creel}$ value obtained for the creels with the average mesh size 34.89 mm and the opening
370 angle 82.15° was 26.9 mm (95% CI: 26.1-27.5). The low estimated SR_{creel} value of 1.24 mm
371 and its narrow confidence intervals (95% CI: 0.62-1.70), as well as the narrow 95% CI of the
372 $CL50_{creel}$ demonstrate a sharp and precise size selection on the seabed. This is expected since
373 the netting is firmly mounted on the creel frame, avoiding a large variation of mesh opening
374 angles as observed in some other creel shapes, such as conical creels (Herrmann et al. 2021).
375 The consequence of having a sharp size selection means that a simple adjustment of mesh size
376 can yield the desired change in the size selection and, therefore, the creel exploitation pattern.

377 Compared to the $CL50_{creel} = 31.8$ mm (95% CI: 17.8–33.2) obtained by Brčić et al. (2018a) for
378 the *Nephrops* creels with the 41 mm square mesh netting, the $CL50_{creel}$ obtained in this study
379 was significantly smaller (i.e., there was no overlap between the 95% CIs). The $CL50_{creel}$
380 obtained in this study was significantly larger than the *Nephrops* *MCRS* (=20 mm CL),
381 indicating a significant mismatch with the desired exploitation pattern. Although the $CL50_{creel}$
382 was significantly larger than *MCRS* and the CL of all *Nephrops* individuals retained by the test
383 creels were above *MCRS*, discarding still occurred. The reason for discarding was not the
384 regulation, since the estimated $CL50_{fisher}$ of 29.62 mm (95% CI: 29.46 – 29.77) was significantly
385 higher than *MCRS*, but, according to the fisher (G. Peranić, pers. comm.), because of the low
386 commercial value of small *Nephrops*. Catchpole et al. (2005) reported that *Nephrops* discarding
387 is strongly influenced by market forces, unlike by quotas or *MCRS*s. The small estimated SR_{fisher}
388 parameter value of 1.31 mm and its narrow confidence intervals (95% CI: 1.08 – 1.51)
389 demonstrate a sharp and precise fisher size selection despite the limited time available to the
390 fisher during creel retrieval to evaluate the size of each *Nephrops* before deciding whether they
391 are going to be landed or discarded. It should be noted that fisher size selection in this study
392 has been estimated for only one fisher and could differ among the fishers. Further, some
393 variation in fisher size selection could potentially be observed throughout the fishing season,
394 and depending on the market value of *Nephrops*.

395 The results obtained showed how the escape, discard and landing probability in creels depend
396 not only on the mesh size but also on the mesh opening angle. However, within the opening
397 angle range of 81° - 90°, falling within the $\pm 10\%$ deviation from perfect square mesh shape,
398 the exploitation pattern ($nP+$, $nP-$) and discard indicators ($nDRatio$, Dp_{max}) were relatively
399 constant. Some caution must be taken knowing that our predictions are based on the *Nephrops*

400 size distribution found during the experimental fishing within a specific area and it can differ
401 spatially and temporally throughout the Adriatic Sea.

402 The Croatian regulation (NN 84/2015) defines 36 mm or 40 mm square mesh as the minimum
403 mesh size in the *Nephrops* creel fishery. Compared to 40 mm square mesh, our results predict
404 that 36 mm mesh size retains more *Nephrops* below the desired fisher size ($CL50_{fisher} = 29.62$
405 mm), resulting in a higher discarding ratio. The unwanted sizes of *Nephrops* could escape from
406 the creels while on the seabed if a larger mesh size (40 mm) was used. This would decrease
407 sorting time onboard the fishing vessel and the probability of unintended *Nephrops* mortality
408 since the high air and sea surface temperatures during fishing impact the survival rate of
409 discarded *Nephrops* (Campos et al. 2015; Albalat et al. 2016; Fox et al. 2020; García-De-
410 Vinuesa et al. 2020). The released individuals are also at risk of being attacked by sea birds
411 (Evans et al. 1994; Eskelund et al. 2019) and other predators on their way to the seabed.
412 Furthermore, knowing the gear and fisher size selection allows fisheries managers to reduce the
413 unwanted discarding practice and easily compare different technological solutions
414 implemented in a fishery.

415

416 ***Acknowledgments***

417 The authors would like to thank Captain Gordan Peranić, crew members Šime Matijević and
418 Lovre Denona for their help during the fieldwork and data collection on board the commercial
419 fishing vessel. We would also like to express our gratitude to Josip Baričević, Ivana Birčić,
420 Petar Crmarić and Marija Torić who helped us construct the control creels. We would also like
421 to thank Jenko Franceschi, Vicko Bašić and Milan Lončar for helping us measure the mesh size
422 of the creel netting. The authors are grateful to Ema Sandalić and Kristine Cerbule for language
423 revision to the anonymous reviewer for the suggestions, which helped us to improve the

424 manuscript significantly. Financial support was provided by the Student Union of the
425 University of Split.

426 ***Competing Interests statement***

427 The authors declare there are no competing interests.

428 ***Data Availability statement***

429 Data generated or analyzed during this study are available from the corresponding author upon
430 reasonable request.

431 ***References***

432 Adey, J.M. 2007. Aspects of the sustainability of creel fishing for Norway lobster, *Nephrops*
433 *norvegicus* (L.), on the west coast of Scotland. PhD thesis. University of Glasgow, 474
434 p.

435 Albalat, A., Collard, A., Brucem, C., Coates, C. J., and Fox, C. J. 2016. Physiological condition,
436 short-term survival, and predator avoidance behavior of discarded Norway lobsters
437 (*Nephrops norvegicus*). *J. Shellfish Res.* **35(4)**: 1053-1065.
438 <https://doi.org/10.2983/035.035.0428>

439 Brčić, J., Herrmann, B., Mašanović, M., Baranović, M., Krstulović Šifner, S., and Škeljo, F.
440 2018a. Size selection of *Nephrops norvegicus* (L.) in commercial creel fishery in the
441 Mediterranean Sea. *Fish. Res.* **200**: 25-32.
442 <https://doi.org/10.1016/j.fishres.2017.12.006>.

443 Brčić, J., Herrmann, B., Mašanović, M., Krstulović Šifner, S., and Škeljo, F. 2018b.
444 CREELSELECT—A method for determining the optimal creel mesh: Case study on

- 445 Norway lobster (*Nephrops norvegicus*) fishery in the Mediterranean Sea. Fish. Res.
446 **204**: 433-440. <https://doi.org/10.1016/j.fishres.2018.03.020>
- 447 Brčić, J., Herrmann, B., and Sala, A. 2018c. Predictive models for codend size selectivity for
448 four commercially important species in the Mediterranean bottom trawl fishery in
449 spring and summer: Effects of codend type and catch size. PLoS ONE 13, e0206044.
450 <https://doi.org/10.1371/journal.pone.0206044>
- 451 Campitelli, E. 2021. metR: Tools for Easier Analysis of Meteorological Fields.
452 doi: 10.5281/zenodo.2593516, R package version 0.12.0.
453 <https://github.com/eliocamp/metR>
- 454 Campos, A., Fonseca, P., Pilar-Fonseca, T., Leocádio, A.M., and Castro, M. 2015. Survival of
455 trawl-caught Norway lobster (*Nephrops norvegicus* L.) after capture and release
456 Potential effect of codend mesh type on survival. Fish. Res. **172**: 415-422.
457 <https://doi.org/10.1016/j.fishres.2015.07.038>
- 458 Catchpole, T.L, Frid, C.L.J., and Gray, T.S. 2005. Discarding in the English north-east coast
459 *Nephrops norvegicus* fishery: the role of social and environmental factors. Fish. Res.
460 **72 (1)**: 45-54. <https://doi.org/10.1016/j.fishres.2004.10.012>
- 461 Commission Delegated Regulation (EU) 2018/2036 of 18 October 2018 amending Delegated
462 Regulation (EU) 2017/86 establishing a discard plan for certain demersal fisheries in
463 the Mediterranean Sea. Official Journal of the European Union L 327.
- 464 Council Regulation (EC) No 1967/2006 of 21 December 2006, concerning management
465 measures for the sustainable exploitation of fishery resources in the Mediterranean
466 Sea, amending Regulation (EEC) No 2847/93 and repealing Regulation (EC) No
467 1626/94. Official Journal of the European Union L. 409.

- 468 Croatian Regulation NN 84/2015. 2015. Pravilnik o obavljanju gospodarskog ribolova na moru
469 mrežama stajaćicama, klopkastim, udičarskim i probodnim ribolovnim alatima te
470 posebnim načinima ribolova. Narodne novine br. 84.
- 471 Efron, B. 1982. The jackknife, the bootstrap and other resampling plans. Society for industrial
472 and applied mathematics. SIAM Monograph No. 38, CBSM-NSF.
- 473 Eno, N.C., MacDonald, D.S., Kinnear, J.A.M., Amos, S.C., Chapman, C.J., Clark, R.A.,
474 Bunker, F.S.P.D., et al. 2001. Effects of crustacean traps on benthic fauna. ICES
475 J. Mar. Sci. **58**: 11–20. <https://doi.org/10.1006/jmsc.2000.0984>
- 476 Eriksson, S.P. 2006. Differences in the condition of Norway lobsters (*Nephrops norvegicus*
477 (L.)) from trawled and creeled fishing areas. Mar. Biol. Res. **2**: 52-58.
478 <https://doi.org/10.1080/17451000600623803>
- 479 Eskelund, M., Methling, C., Vilhelm Skov, P., and Madsen, N. 2019. Survival of discarded
480 plaice (*Pleuronectes platessa*) from Norway lobster (*Nephrops norvegicus*) otter-trawl
481 fishery. J. Appl. Ichthyol. **35(3)**: 645-654. <https://doi.org/10.1111/jai.13888>
- 482 Evans, S. M., Hunter, J. E., and Wahju, R. I. 1994. Composition and fate of the catch and
483 bycatch in the Farne Deep (North Sea) *Nephrops* fishery. ICES J. Mar. Sci. **51(2)**: 155-
484 168. <https://doi.org/10.1006/jmsc.1994.1017>
- 485 FAO, 2020. The State of Mediterranean and Black Sea Fisheries 2020. General Fisheries
486 Commission for the Mediterranean. Rome. <https://doi.org/10.4060/cb2429en>
- 487 FAO-GFCM, 2021. Fishery and Aquaculture Statistics. GFCM capture production 1970-2019
488 (FishstatJ). In: FAO Fisheries Division [online]. Rome. Updated 2021.
489 www.fao.org/fishery/statistics/software/fishstatj/en.

- 490 Fox, C. J., Albalat, A., Valentinsson, D., Nilsson, H. C., Armstrong, F., Randall, P., and
491 Catchpole, T. 2020. Survival rates for *Nephrops norvegicus* discarded from Northern
492 European trawl fisheries. ICES J. Mar. Sci. **77(5)**: 1698-1710.
493 <https://doi.org/10.1093/icesjms/fsaa037>
- 494 García-De-Vinuesa, A., Breen, M., Benoît, H. P., Maynou, F., and Demestre, M. 2020. Seasonal
495 variation in the survival of discarded *Nephrops norvegicus* in a NW Mediterranean
496 bottom-trawl fishery. Fish. Res. **230**: 105671.
497 <https://doi.org/10.1016/j.fishres.2020.105671>
- 498 Herrmann, B., Sistiaga, M., Nielsen, K.N., and Larsen, R.B. 2012. Understanding the size
499 selectivity of redfish (*Sebastes* spp.) in North Atlantic trawl codends. J. Northwest Atl.
500 Fish. Sci. **44**: 1–13. <http://dx.doi.org/10.2960/J.v44.m680>
- 501 Herrmann, B., Sistiaga, M., Larsen, R.B., Nielsen, K.N., and Grimaldo, E. 2013. Understanding
502 sorting grid and codend size selectivity of Greenland halibut (*Reinhardtius*
503 *hippoglossoides*). Fish. Res. **146**: 59-73. <https://doi.org/10.1016/j.fishres.2013.04.004>
- 504 Herrmann, B., Grimaldo, E., Brčić, J., and Cerbule, K. 2021. Modelling the effect of mesh size
505 and opening angle on size selection and capture pattern in a snow crab (*Chionoecetes*
506 *opilio*) pot fishery. Ocean Coast. Manage. **201**: 105495.
507 <https://doi.org/10.1016/j.ocecoaman.2020.105495>
- 508 Hill, A. E., and White, R. G. 1990. The dynamics of Norway lobster (*Nephrops norvegicus* L.)
509 populations on isolated mud patches. ICES J. Mar. Sci. **46(2)**: 167-174.
510 <https://doi.org/10.1093/icesjms/46.2.167>
- 511 Johnson, M. P., Lordan, C., and Power, A. M. 2013. Habitat and ecology of *Nephrops*
512 *norvegicus*. In Advances in Marine Biology, pp. 27-63. Ed. M.L. Johnson, and M.P.

- 513 Johnson. Academic Press, 325 p. [https://doi.org/10.1016/B978-0-12-410466-2.00002-](https://doi.org/10.1016/B978-0-12-410466-2.00002-9)
514 [9](https://doi.org/10.1016/B978-0-12-410466-2.00002-9)
- 515 Kalogirou, S., Pihl, L., Maravelias, C.D., Herrmann, B., Smith, C.J., Papadopoulou, N., Notti,
516 E., et al. 2019. Shrimp trap selectivity in a Mediterranean small-scale-fishery. Fish.
517 Res. **211**: 131–140. <https://doi.org/10.1016/j.fishres.2018.11.006>
- 518 Kopp, D., Coupeau, Y., Vincent, B., Morandeau, F., Méhault, S., and Simon, J. 2020. The low
519 impact of fish traps on the seabed makes it an ecofriendly fishing technique. PLoS
520 ONE 15(8), e0237819. <https://doi.org/10.1371/journal.pone.0237819>
- 521 Larsen, R.B., Sistiaga, M., Herrmann, B., Brinkhof, J., Tatone, I., and Santos, J. 2018. The
522 effect of Nordmøre grid length and 1 angle on codend entry of bycatch fish species
523 and shrimp catches. Can. J. Fish. Aquat. Sci. **76(2)**: 308-319.
524 <https://doi.org/10.1139/cjfas-2018-0069>
- 525 Lolas, A., and Vafidis, D. 2021. Population Dynamics, Fishery, and Exploitation Status of
526 Norway Lobster (*Nephrops norvegicus*) in Eastern Mediterranean. Water, **13(3)**: 289.
527 <https://doi.org/10.3390/w13030289>
- 528 Melli, V., Herrmann, B., Karlsen, J.D., Feekings, J.P., and Krag, L.A. 2020. Predicting optimal
529 combinations of bycatch reduction devices in trawl gears: a meta-analytical approach.
530 Fish Fish. **21(2)**: 252–268. <https://doi.org/10.1111/faf.12428>
- 531 Morello, E.B., Antolini, B., Gramitto, M.E., Atkinson, R.J.A., and Froggia, C. 2009. The fishery
532 for *Nephrops norvegicus* (Linnaeus, 1758) in the central Adriatic Sea (Italy):
533 Preliminary observations comparing bottom trawl and baited creels. Fish. Res. **95**:
534 325-331. <https://doi.org/10.1016/j.fishres.2008.10.002>

- 535 Mytilineou, C., Herrmann, B., Mantopoulou-Palouka, D., Sala, A., and Megalofonou, P. 2018.
536 Modelling gear and fishers size selection for escapees, discards, and landings: a case
537 study in Mediterranean trawl fisheries. *ICES J. Mar. Sci.* **75(5)**: 1693-1709.
538 <https://doi.org/10.1093/icesjms/fsy047>
- 539 Mytilineou, C., Herrmann, B., Kavadas, S., Smith, C., and Megalofonou, P. 2020. Combining
540 selection models and population structures to inform fisheries management: a case
541 study on hake in the Mediterranean bottom trawl fishery. *Mediterr. Mar. Sci.* **21(2)**:
542 360-371. <https://doi.org/10.12681/mms.22191>
- 543 Mytilineou, C., Herrmann, B., Mantopoulou-Palouka, D., Sala, A., and Megalofonou, P. 2021a.
544 Escape, discard, and landing probability in multispecies Mediterranean bottom-trawl
545 fishery. *ICES J. Mar. Sci.* <https://doi.org/10.1093/icesjms/fsab048>
- 546 Mytilineou, C., Herrmann, B., Sala, A., Mantopoulou-Palouka, D. and Megalofonou, P. 2021b.
547 Estimating overall size-selection pattern in the bottom trawl fishery for four
548 economically important fish species in the Mediterranean Sea Ocean Coast. *Manage.*
549 **209**: 105653. <https://doi.org/10.1016/j.ocecoaman.2021.105653>
- 550 Olsen, L., Herrmann, B., Sistiaga, M., and Grimaldo, E. 2019. Effect of gear soak time on size
551 selection in the snow crab pot fishery. *Fish. Res.* **214**: 157-165.
552 <https://doi.org/10.1016/j.fishres.2019.02.005>
- 553 Petetta, A., Virgili, M., Guicciardi, S., and Lucchetti, A. 2021. Pots as alternative and
554 sustainable fishing gears in the Mediterranean Sea: an overview. *Rev. Fish Biol.*
555 *Fisher.* **31(4)**: 773-795. <https://doi.org/10.1007/s11160-021-09676-6>
- 556 R Core Team, 2021. R: A language and environment for statistical computing. R Foundation
557 for Statistical Computing, Vienna, Austria. <https://www.R-project.org/>.

- 558 Regulation (EU) No 1380/2013, of the European Parliament and of the Council of 11 December
559 2013 on the Common Fisheries Policy, amending Council Regulations (EC) No
560 1954/2003 and (EC) No 1224/2009 and repealing Council Regulations (EC) No
561 2371/2002 and (EC) No 639/2004 and Council Decision 2004/585/EC. Official
562 Journal of the European Union L 354.
- 563 Ridgway, I.D., Taylor, A.C., Atkinson, R.J.A., Chang, E.S., and Neil, D.M. 2006. Impact of
564 capture method and trawl duration on the health status of the Norway lobster,
565 *Nephrops norvegicus*. J. Exp. Mar. Biol. Ecol. **339**: 135-147.
566 <https://doi.org/10.1016/j.jembe.2006.07.008>
- 567 Sala, A., Herrmann, B., De Carlo, F., Lucchetti, A., Brčić, J. 2016. Effect of codend
568 circumference on the size selection of square-mesh codends in trawl fisheries. PloS
569 One 11 (7), e0160354. <https://doi.org/10.1371/journal.pone.0160354>.
- 570 Sistiaga, M., Herrmann, B., Grimaldo, E., and O'Neill, F.G. 2016. Estimating the selectivity of
571 unpaired trawl data: a case study with a pelagic gear. Sci. Mar. **80**: 321-
572 327. <http://dx.doi.org/10.3989/scimar.04409.26B>
- 573 Thomsen, B., Humborstad, O.B., and Furevik, D.M. 2010. Fish Pots: Fish Behavior, Capture
574 Processes, and Conservation Issues. In Behavior of Marine Fishes Capture Processes
575 and Conservation Challenges, pp. 143-154. Ed. by He P. Blackwell Publishing Ltd.,
576 Iowa, 375 p.
- 577 Wickham, H. 2016. ggplot2: Elegant Graphics for Data Analysis. Springer-Verlag New York.
578 ISBN 978-3-319-24277-4. <https://ggplot2.tidyverse.org>
- 579 Wienbeck, H., Herrmann, B., Feekings, J.P., Stepputtis, D., and Moderhak, W. 2014. A
580 comparative analysis of legislated and modified Baltic Sea trawl codends for
581 simultaneously improving the size selection of cod (*Gadus morhua*) and plaice

- 582 (*Pleuronectes platessa*). Fish. Res. **150**: 28–37.
 583 <https://doi.org/10.1016/j.fishres.2013.10.007>
- 584 Wileman, D., Ferro, R.S.T., Fonteyne, R., and Millar, R.B. 1996. Manual of methods of
 585 measuring the selectivity of towed fishing gears. ICES Coop. Res. Rep. No. 215.
- 586 Winger, P.D., and Walsh, P.J. 2007. The feasibility of escape mechanisms in conical snow crab
 587 traps. ICES J. Mar. Sci. **64**: 1587-1591.
- 588 Winger, P. D., and Walsh, P. J. 2011. Selectivity, efficiency, and underwater observations of
 589 modified trap designs for the snow crab (*Chionoecetes opilio*) fishery in
 590 Newfoundland and Labrador. Fish. Res. **109(1)**: 107-113.
 591 <https://doi.org/10.1016/j.fishres.2011.01.025>
- 592 Xu, X., and Millar, R. B. 1993. Estimation of trap selectivity for male snow crab (*Chionoecetes*
 593 *opilio*) using the SELECT modeling approach with unequal sampling effort. Can. J.
 594 Fish. Aquat. Sci. **50(11)**: 2485-2490. <https://doi.org/10.1139/f93-273>

595

596 **Tables**

597 **Table 1.** Number of creels and longlines deployed and number of *Nephrops* caught (N) in test
 598 and control creels on each fishing day.

Date	Configuration	Num of creels	Num of longlines	Soak time (days)	N
05 April 2019	test	266	8	2	418
	control	30	1	2	35
06 April 2019	test	266	8	1	402
	control	30	1	1	35
17 April 2019	test	266	8	1	402

18 April 2019	test	266	8	1	440
	control	30	1	1	54
20 April 2019	test	266	8	2	470
	control	30	1	2	49
30 April 2019	test	137	4	2	221
	control	29	1	2	36
01 May 2019	test	137	4	1	207
	test	129	4	3	187
	control	29	1	1	43
02 May 2019	test	266	8	1	428
	control	27	1	1	48
04 June 2019	test	266	8	1	389
	control	29	1	1	53
05 June 2019	test	96	3	1	130
07 June 2019	test	64	2	2	75
	test	169	5	3	268
	control	29	1	3	48
08 June 2019	test	266	8	1	397
	control	29	1	1	55
12 June 2019	test	266	8	4	428
	control	29	1	4	63
14 June 2019	test	266	8	2	434
	control	29	1	2	45
19 June 2019	test	266	8	4	434
	control	29	1	4	43
21 June 2019	test	266	8	2	396
	control	29	1	2	55
04 July 2019	test	266	8	2	468
	control	29	1	2	50

600

601 **Table 2.** Size selection parameters obtained for *Nephrops* in creels soaked for one (S1), two
 602 (S2), three (S3), four (S4) days soak time and logit model fit statistics. Values in () represent
 603 95% Efron confidence intervals. *CL50*: CL at which 50% of the *Nephrops* are retained (mm);
 604 *SR*: selection range (mm); *SP*: split parameter; DOF: degrees of freedom.

	S1	S2	S3	S4
<i>CL50</i>	27.13 (25.82-27.95)	26.57 (25.13-27.86)	25.61 (25.11-28.20)	27.28 (25.59-27.81)
<i>SR</i>	1.57 (0.10-2.47)	0.98 (0.10-2.21)	0.1 (0.10-1.61)	1.1 (0.10-1.50)
<i>SP</i>	0.92 (0.91-0.94)	0.92 (0.91-0.94)	0.91 (0.90-0.93)	0.93 (0.89-0.96)
<i>p</i> -value	0.84	0.51	0.46	0.33
Deviance	9.65	15.27	13.9	17.81
DOF	15	16	14	16

605

606

607 **Table 3.** Creel size selectivity parameters, fisher size selectivity parameters, logit model fit
 608 statistics for creel and fishers size selection and discard indicators. DOF: degrees of freedom.
 609 Values in () represent 95% Efron confidence intervals. *CL50_{creel}*: CL at which 50% of the
 610 *Nephrops* are retained by the creel (mm); *SR_{creel}*: creel selection range (mm); *SP*: split factor;
 611 *CL50_{fisher}*: CL at which 50% of the *Nephrops* are retained by the fisher (mm); *SR_{fisher}*: fisher
 612 selection range (mm); *LDp_{max}* represents the CL of *Nephrops* (mm) where maximum discarding
 613 probability (*Dp_{max}*) occurs; *DR_x* represents the CL range (mm) where discarding probability is
 614 at least x%, where x = (5%, 25%, 50%, 75%, 95%).

Parameter	Value (CI)
<i>CL50_{creel}</i>	26.94 (26.10-27.49)
<i>SR_{creel}</i>	1.24 (0.62-1.70)
<i>SP</i>	0.92 (0.91 - 0.93)
<i>p</i> -value _{creel}	0.5991
Deviance _{creel}	15.91
DOF _{creel}	18

$CL50_{fisher}$	29.62 (29.46 - 29.77)
SR_{fisher}	1.31 (1.08 - 1.51)
$p\text{-value}_{fisher}$	<0.001
Deviance $_{fisher}$	138.53
DOF $_{fisher}$	43
$DR_{0.05}$	60.11 (55.71 - 66.32)
$DR_{0.25}$	39.54 (34.92 - 45.26)
$DR_{0.50}$	26.55 (19.98 - 35.18)
$DR_{0.75}$	12.31 (0.00 - 25.10)
$DR_{0.95}$	00.0 (0.00 - 07.87)
Dp_{max}	0.83 (0.70 - 0.97)
LDp_{max}	28.26 (27.43 - 28.60)

615

616 **Figure Captions**

617 **Figure 1.** Map of the study area. The green dots represent test longlines while the red dots
 618 represent control longlines. The map was created using QGIS version 3.22.7., with basemaps
 619 from Google Satellite 2022.

620

621 **Figure 2.** Catch sharing and size selection curves (solid) with their respective 95% confidence
 622 intervals (dashed) for one (S1), two (S2), three (S3) and four (S4) day soak time.

623

624 **Figure 3.** Catch sharing and size selection curves (solid) with their respective 95% confidence
 625 intervals (dashed) for all soak times pooled together. Vertical grey dotted line represents
 626 *Nephrops* minimum conservation reference size (MCRS = 20 mm CL)

627

628 **Figure 4.** Fishermen size selection curve (solid black line) with 95% Efron confidence intervals
629 (dashed black lines). Vertical grey dotted line represents *Nephrops* minimum conservation
630 reference size (MCRS = 20 mm CL).

631

632 **Figure 5.** The length-dependent escape (solid green line), discard (solid red line), and landing
633 probability (solid blue line) and their respective 95% Efron confidence intervals (dashed lines).
634 Vertical grey dotted line represents *Nephrops* minimum conservation reference size (MCRS =
635 20 mm CL).

636

637 **Figure 6.** Predicted escape (green), discard (red) and landing (blue) curves for different mesh
638 sizes and mesh opening angles. MS: mesh size; OA: mesh opening angle.

639

640 **Figure 7.** Iso-lines showing predicted maximum discard probability values for creels with
641 different mesh sizes and mesh opening angles (OA). The solid black dot represents the
642 maximum discard probability obtained for the experimental creels in this study.

643

644 **Figure 8.** Iso-lines showing predicted exploitation pattern indicator values (np^- , np^+ , $nDRatio$)
645 for a range of mesh sizes and opening angles. The black solid dots represent the indicator values
646 obtained for the experimental creels in this study. Vertical dotted lines indicate the two legal
647 mesh sizes (36 and 40 mm) allowed in the Croatian *Nephrops* creel fishery.

648

649

650

651

652

653

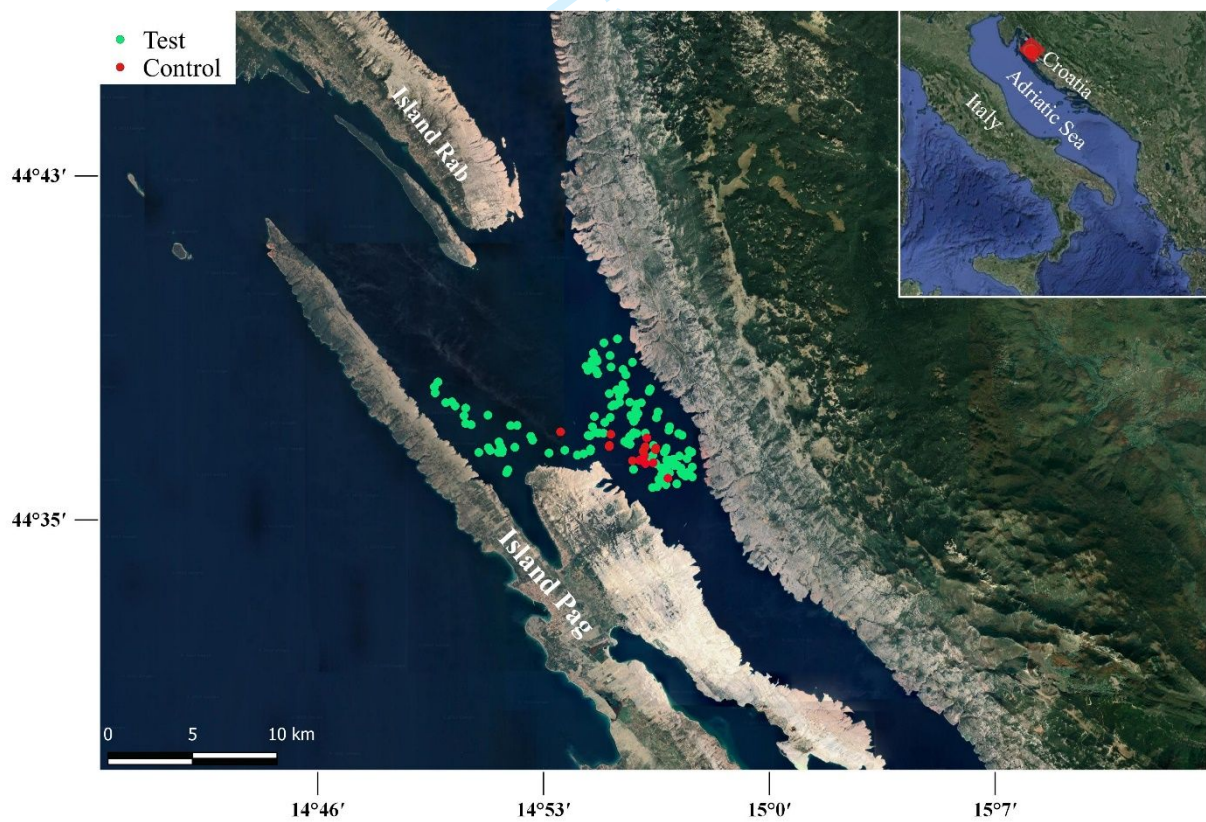
654

655

656

657 **Figures**

658 Figure 1.



659

660

661

662

663

664

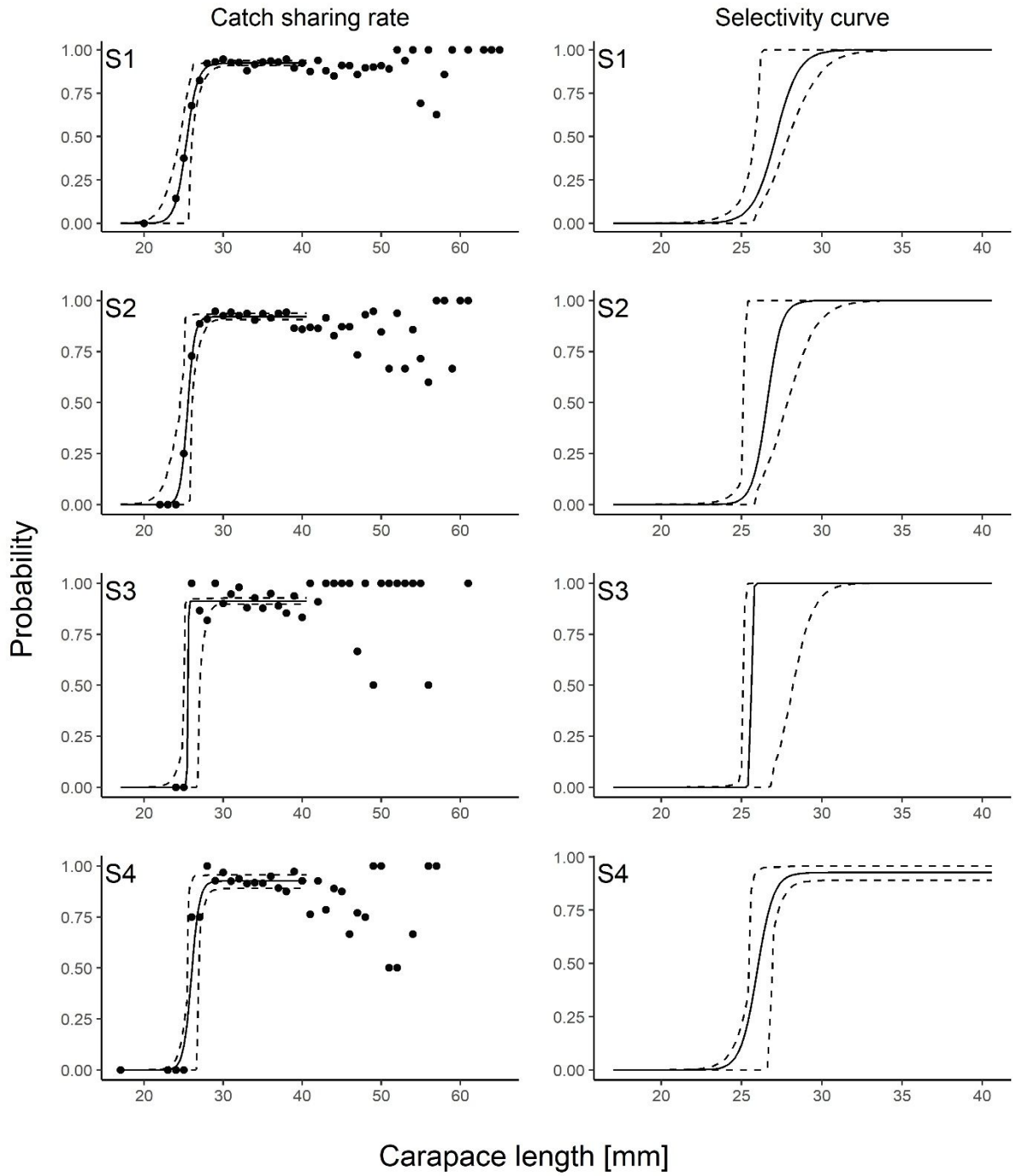
665

666

667

668 Figure 2.

Draft



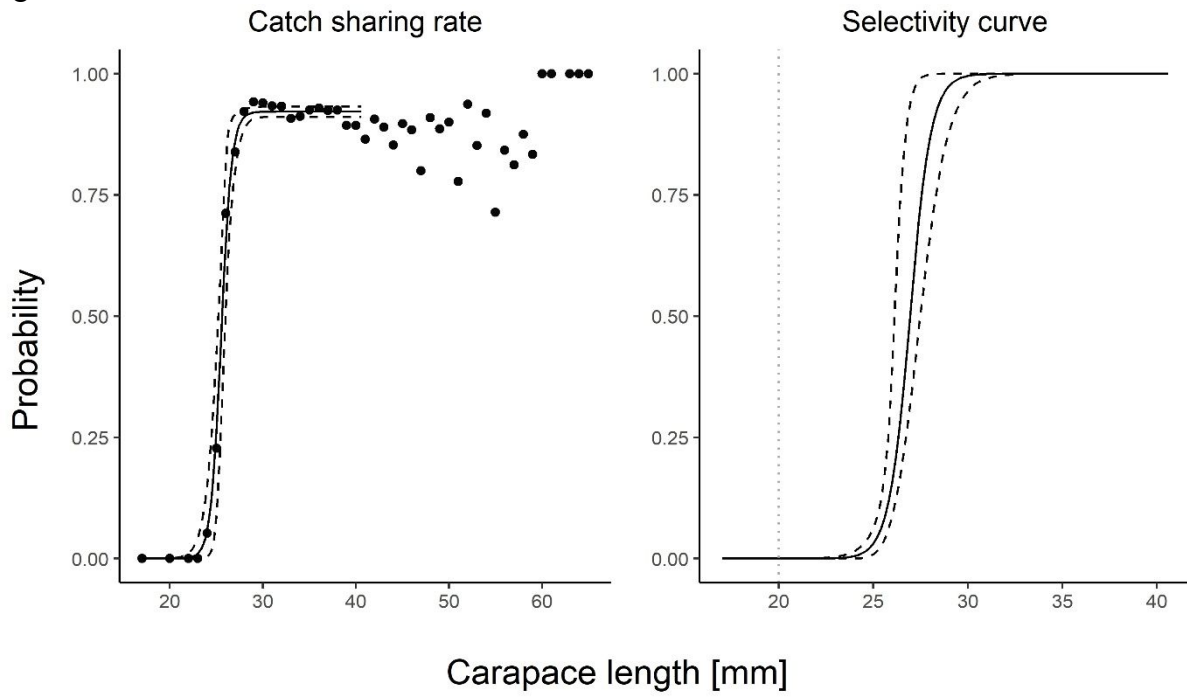
669

670

671

672

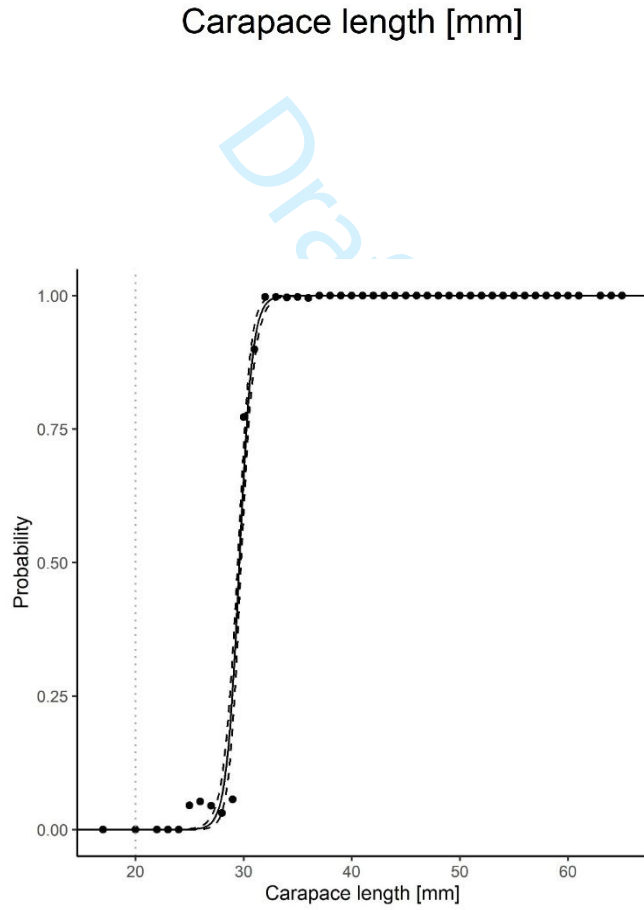
673 Figure 3.



674

675 Figure 4.

676

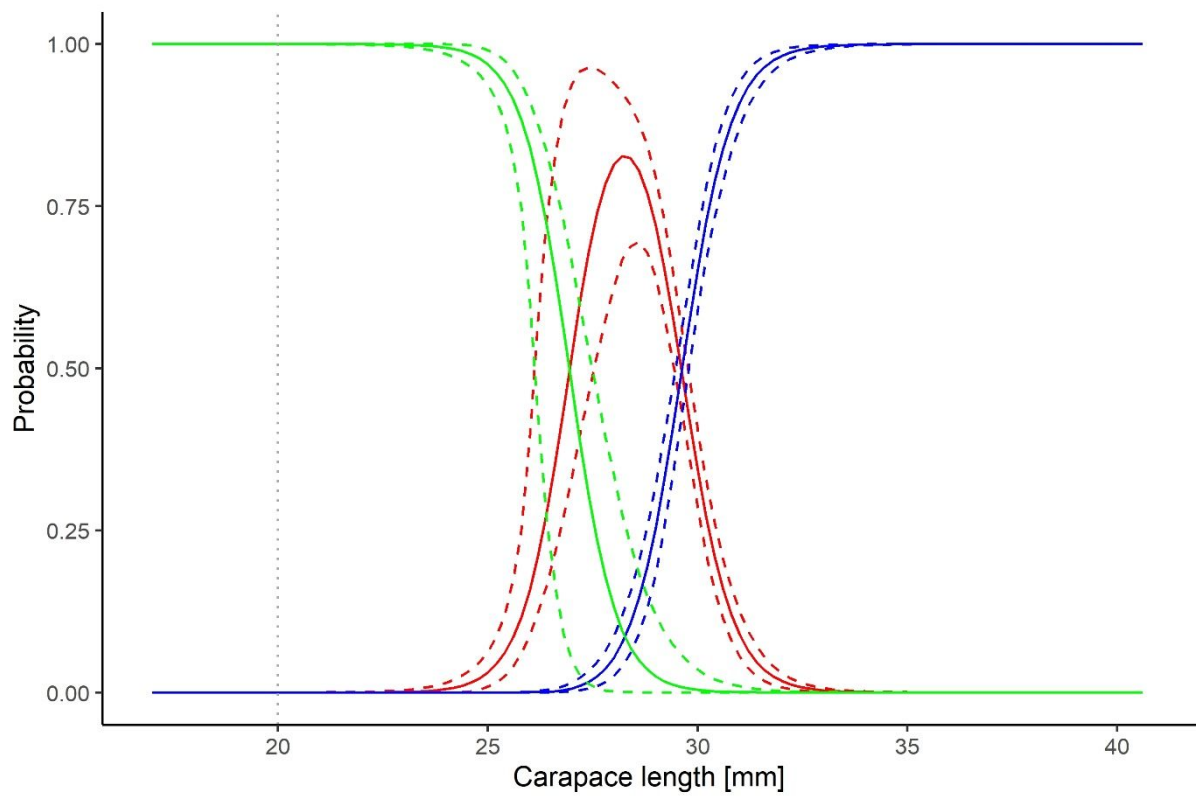


677

678

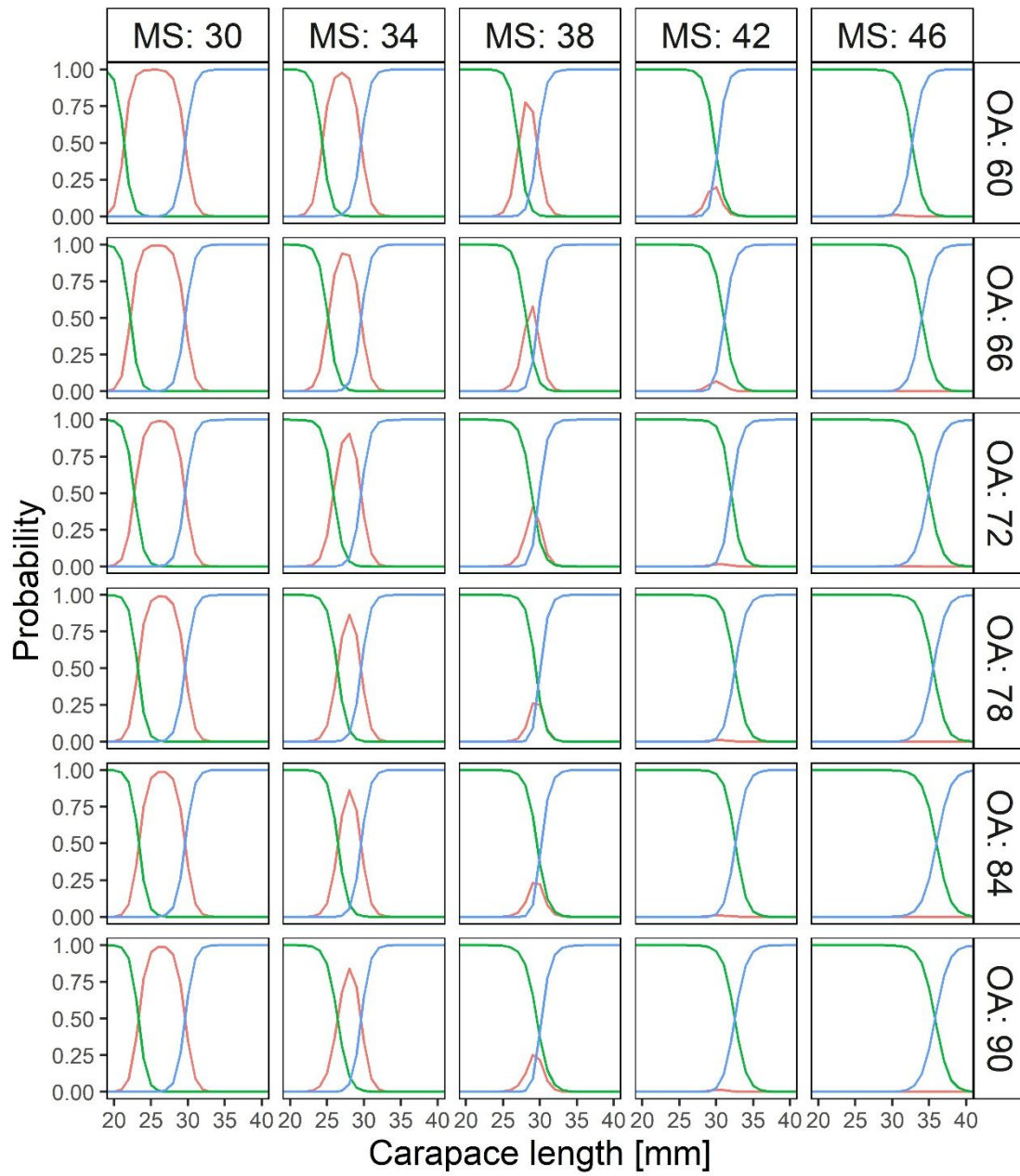
679

680 Figure 5.



681
682
683
684
685
686
687
688
689
690
691
692
693

Figure 6.



694

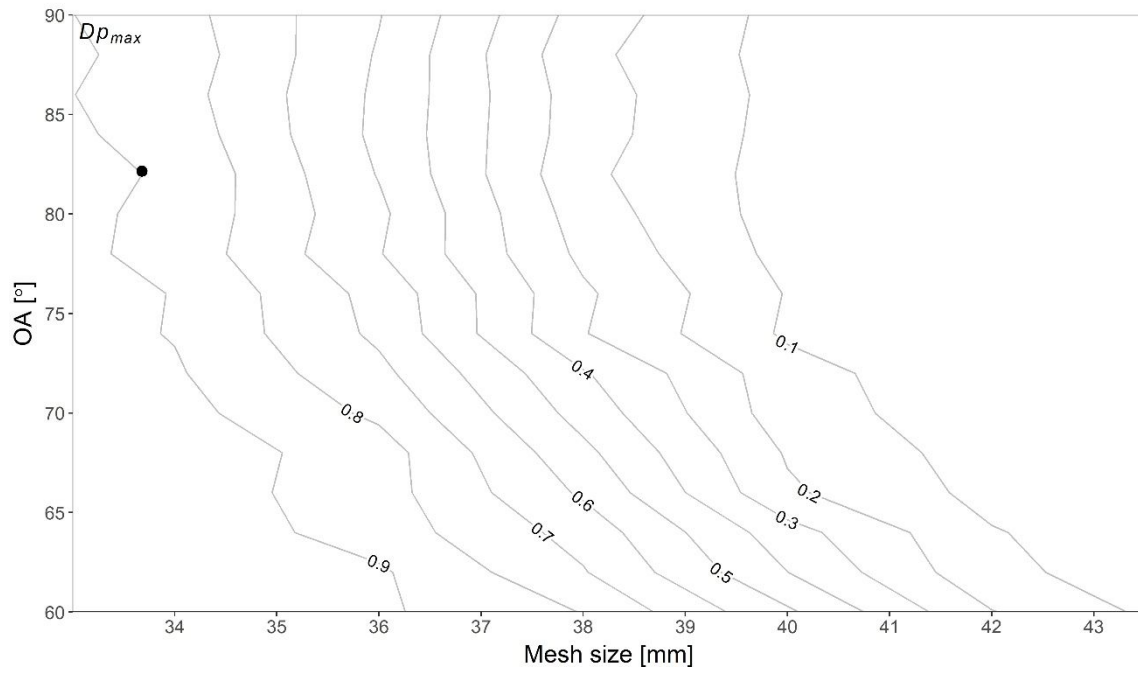
695

696

697

698

699 Figure 7.



700

701

702

703

704

705

706

707

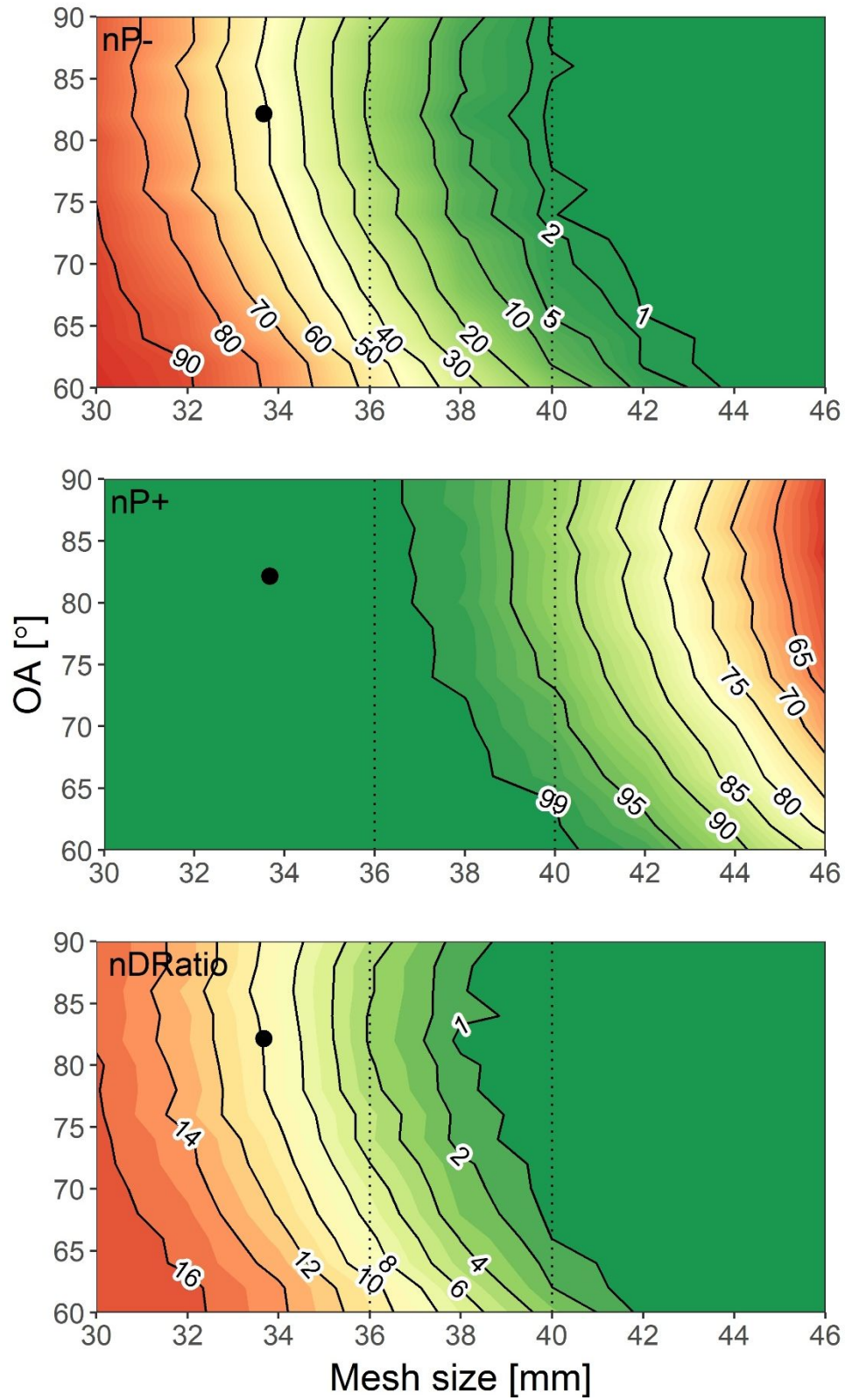
708

709

710

711 Figure 8.

Draft



712